MAUSAM, **77**, 3 (July 2026), 777-790

MAUSAM

DOI: https://doi.org/10.54302/mausam.v77i3.6965
Homepage: https://mausamjournal.imd.gov.in/index.php/MAUSAM

UDC No.551.583.16:551.524:551.508.8(540.49)

Heatwave mapping using satellite-derived LST in Western Madhya Pradesh, India

GAURAVENDRA. P. SINGH*, ADARSH DUBE, NEETIN NARKHEDE and G. K. SAWAISARJE

India Meteorological Department, Pune, 411005, India.

(*Received 10 February 2025, Accepted 7 August 2025*)

***Corresponding author's email: gauravendra.singh@gmail.com**

सार – भारत की लगभग 60% आबादी हर साल 10 से 20 दिनों के लिए ऐसे अत्यधिक तापमान के संपर्क में आती है जो स्वास्थ्य जोखिम के महत्वपूर्ण स्तरों को पार कर जाता है। हालांकि, देश के विभिन्न भौगोलिक क्षेत्रों में गर्मी का वितरण और उससे जुड़ी संवेदनशीलताएं काफी भिन्न हैं, जिससे उच्च जोखिम वाले क्षेत्रों की पहचान करना चुनौतीपूर्ण हो जाता है। इन हॉटस्पॉट्स को पहचानना और निर्णय लेने की प्रक्रियाओं में जोखिम प्रबंधन प्रणालियों को एकीकृत करने के लिए एक व्यापक ढांचा स्थापित करना अत्यंत महत्वपूर्ण है। विशेष रूप से, ग्रीष्म लहरों (Heatwaves) के प्रति संवेदनशील क्षेत्रों में आगे के अनुसंधान के महत्व पर प्रकाश डालने के लिए सीमा मान डिटेक्शन (देहली पहचान) विधियों पर ध्यान केंद्रित करने की आवश्यकता है। इस अध्ययन में मध्य भारत के पश्चिमी मध्य प्रदेश में 2009 और 2020 के बीच घटित 33 ग्रीष्म लहर की घटनाओं का विश्लेषण करने के लिए भारत मौसम विज्ञान विभाग (IMD) के दैनिक माध्य ग्रिडेड सतही वायु तापमान डेटा के साथ MODIS लैंड सरफेस टेम्परेचर (LST) डेटा का उपयोग किया गया। निष्कर्ष प्रदर्शित करते हैं कि सैटेलाइट-व्युत्पन्न LST डेटा प्रभावी रूप से क्षेत्रीय ग्रीष्म लहर के प्रतिरूपों की पहचान कर सकता है, जिसमें वायु तापमान विसंगतियों के माध्यम से खोजी गई ग्रीष्म लहरों और LST विचलन का उपयोग करके अनुमानित ग्रीष्म लहरों के बीच एक मजबूत सहसंबंध (सहसंबंध गुणांक लगभग 0.7) देखा गया है। इसके अलावा, अध्ययन ने ग्रीष्म लहर की पहचान के लिए इष्टतम LST सीमा मान स्थापित किए: सामान्य ग्रीष्म लहरों के लिए 70वां पर्सेंटाइल (52.5°C) और गंभीर ग्रीष्म लहरों के लिए 90वां पर्सेंटाइल (53.5°C)। इसके अतिरिक्त, परिणाम उत्तरी और मध्य भारत में गर्मियों के गर्म होने की एक स्पष्ट प्रवृत्ति को इंगित करते हैं, जिससे पिछले दशक में ग्रीष्म लहरों की आवृत्ति, तीव्रता और अवधि में वृद्धि हुई है।

ABSTRACT. Approximately 60% of India's population is exposed to extreme temperatures that exceed critical health risk thresholds for 10 to 20 days each year. However, the distribution of heat and the associated vulnerabilities vary significantly across the country's physiographical regions, making it challenging to identify high-risk areas. Recognizing these hotspots and establishing a comprehensive framework to integrate risk management systems into decision-making processes is crucial. In particular, there is a need to focus on threshold detection methods to highlight the importance of further research in regions susceptible to heatwaves. This study utilized MODIS Land Surface Temperature (LST) data alongside daily mean gridded surface air temperature data from the India Meteorological Department (IMD) to analyze 33 heatwave events that occurred between 2009 and 2020 in western Madhya Pradesh, central India. The findings demonstrate that satellite-derived LST data can effectively identify regional heatwave patterns, with a strong correlation (correlation coefficient approximately 0.7) observed between heatwaves detected via air temperature anomalies and those estimated using LST departures. Furthermore, the study established optimal LST thresholds for heatwave detection: the 70th percentile (52.5 °C) for standard heatwaves and the 90th percentile (53.5 °C) for severe heatwaves. Additionally, the results indicate a noticeable trend of summer warming in northern and central India, leading to increased heatwaves' frequency, intensity, and duration over the past decade.

Key words – Land surface temperature, mortality, MODIS, IMD, heat wave.

1. Introduction

Heatwave events profoundly impact human activities and natural ecosystems, adversely affecting human health, inhibiting vegetation growth, and disrupting livestock processes (Zhang *et al*., 2016; Li *et al*., 2017). Projections from global climate models suggest that the intensity and consequences of heatwaves will escalate in the 21st century due to ongoing climate warming (Mora *et al*., 2017; Dosio *et al*., 2018). Historical events illustrate the severity of such occurrences: the 2003 European heatwave resulted in approximately 70,000 excess deaths (Robine *et al*., 2008), while the 2010 Russian heatwave caused significant casualties, extensive crop failures, the

destruction of millions of hectares of land, and substantial economic losses (Barripedro *et al*., 2011; Trenberth *et al*., 2012). In South Asia, the 2010 Ahmedabad heatwave led to over 1,300 fatalities, prompting the development of the region's first coordinated heat action plans (Knowlton *et al*., 2014).

Accurately mapping the spatial extent of heatwaves remains challenging due to the limited distribution of meteorological stations, particularly in diverse physiographical regions (Perkins *et al*., 2015). Changes in land use and land cover (LULC) further influence large-scale heatwave variability, yet vegetation and surface moisture conditions often receive insufficient consideration (Findell *et al*., 2017). Land-atmosphere feedback mechanisms exacerbate extreme temperatures, driven by both antecedent and concurrent dry conditions (Russo *et al*., 2019; Ribeiro *et al*., 2020).

In this context, satellite-derived Land Surface Temperature (LST) is a valuable tool for spatiotemporal heatwave analysis, particularly in regions with sparse meteorological networks (Snyder *et al*., 1998; Albright *et al*., 2011). LST is widely recognised as a key indicator in climate change studies, aiding in the computation of sensible and latent heat fluxes and identifying extreme climate events influenced by atmospheric circulation and teleconnections (Jin, 2004). Compared to air temperature, LST provides more detailed insights into the surface energy budget by capturing the Earth's thermal emissions, whereas air temperature data is more suited for assessing relatively homogenous surface conditions (Mildrexler *et al*., 2011; Oyler *et al*., 2016).

Projections for India indicate an increase in air temperature of 3-4 °C by the end of the 21st century, with northern regions expected to experience the most pronounced effects (Chaturvedi *et al*., 2012). Night-time LST and minimum air temperature have demonstrated consistency across different land cover types due to their reduced sensitivity to solar insolation, making them robust indicators for heatwave studies (Good *et al*., 2017).

This study underscores the importance of integrating air temperature and LST data for enhanced heatwave detection in western Madhya Pradesh. Situated between the hot arid climate of Rajasthan to the west and the forested state of Chhattisgarh to the east, the region functions as a climatic transition zone, making it critical for analysing heatwave movement and dynamics. The analysis of maximum LST anomalies from 2003 to 2014 has proven effective in identifying abnormally high temperatures associated with extreme global weather phenomena, including heatwaves, droughts, and land-use changes (Mildrexler *et al*., 2018). For instance, continuous warming trends in western North America from 2002 to 2018, driven by El Niño and La Niña events, revealed significant spatial LST variations (Yan *et al*., 2020). The extreme heatwave in western North America in 2021, characterised by exceptionally high LST and air temperature values, was linked to anthropogenic climate change (Sjoukje *et al*., 2021).

Despite increasing global research on heatwaves, studies specific to India remain limited, with most focusing on climatology and long-term trends (Rohini *et al*., 2016; Pai *et al*., 2013). This research addresses a critical gap by examining heatwave detection in western Madhya Pradesh using high-resolution LST data. A comparative analysis of heatwave detection methods using IMD air temperature and satellite-based LST is presented in Section 4. Additionally, Section 5 outlines threshold LST values for heatwave zones, aligned with air temperature criteria. By integrating high-resolution satellite data with ground-based observations, this study advances the understanding of heatwave dynamics in a region prone to extreme temperatures. The findings contribute to improved risk management and adaptation strategies, supporting efforts to mitigate the escalating impacts of heatwaves in India.

2. Data and methodology

2.1. *Study region*

Western Madhya Pradesh is situated between latitudes 21°4'9.8286"N and 23°56'326"N and longitudes 76°16'48.1038"E to 78°21'23.8608"E, encompassing an area of 17,351.25 km² (Figure 1). The region experiences a semi-arid climate, characterised by hot summers and mild winters. Most of annual precipitation occurs during the monsoon season (June–September). Summers are typically hot and dry, with temperatures reaching 40 °C, while winter temperatures can drop to approximately 10 °C.

Land use and land cover (LULC) changes in the region are influenced by geological, topographical, climatic, and anthropogenic factors, resulting in a heterogeneous landscape comprising agricultural land, forests, grasslands, and urban settlements. The extreme summer temperatures make the region particularly suitable for studying satellite-derived Land Surface Temperature (LST) to assess temperature variability and its implications for the local ecology, economy, and society. Additionally, the availability of LST data enables insights into crop monitoring and management and urban heat island (UHI) studies, particularly in major urban centres such as Indore and Ujjain.

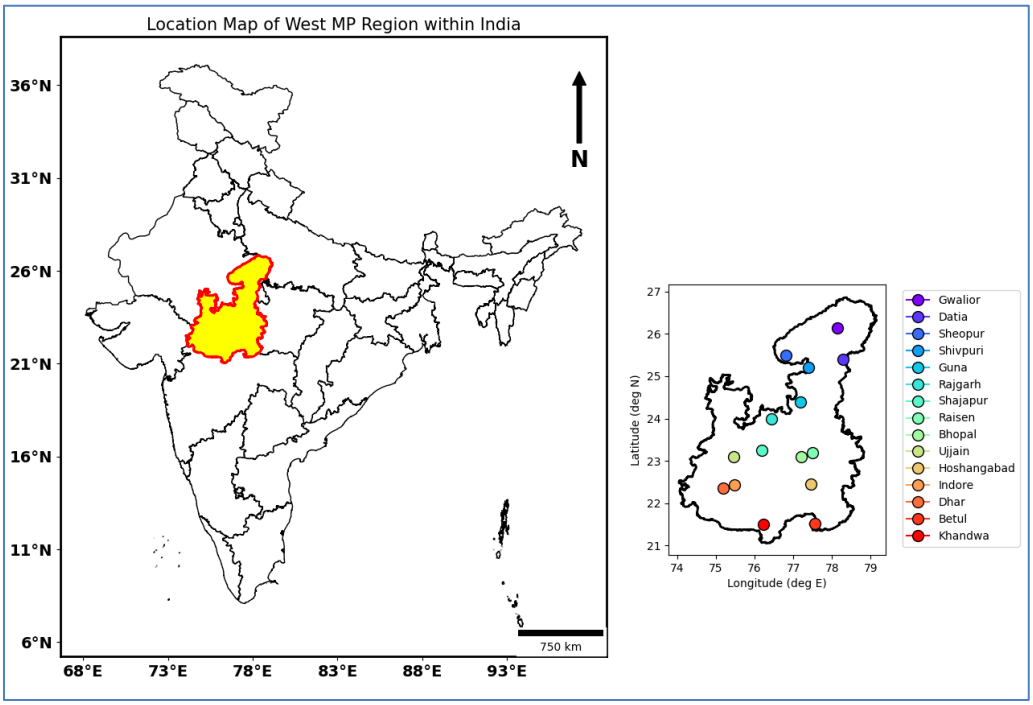

Fig. 1. Map of India is shown (left) along with the study region highlighted in it and the study region is enlarged to the right showing the locations of IMD stations

2.2. *Dataset*

To analyse heatwave characteristics through air temperature variations, this study utilised daily mean gridded surface air temperature data from the India Meteorological Department (IMD) at a spatial resolution of 1° × 1°, covering the period from 1951 to 2020. Data from 15 surface meteorological observatories, maintained by IMD, were used to validate identified heatwave events. Additionally, daily mean surface relative humidity (measured at 2 m) and wind data (at 850 hPa) were obtained from the NCMRWF-IMDAA (Indian Monsoon Data Assimilation and Analysis) reanalysis dataset, which provides a spatial resolution of 12 km and spans from 1979 to 2020.

Air temperature observations were collected from ground-based meteorological stations following World Meteorological Organization (WMO) standards. Measurements were taken at a height of 2 m above ground level and included daily maximum air temperature values. The study incorporated data from 15 meteorological stations located across diverse environmental conditions in western Madhya Pradesh (Fig. 1).

Satellite-based data included Land Surface Temperature (LST) at a spatial resolution of 1 km, derived from the Moderate Resolution Imaging Spectroradiometer (MODIS) sensors aboard the Terra satellite. Terra follows a sun-synchronous orbit, crossing the equator from south to north at approximately 1:30 a.m. local time. The MODIS LST data were processed using the split-window algorithm, which utilizes thermal infrared band channels 31 (10.78–11.28 μm) and 32 (11.77–12.27 μm) (Vancutsem *et al*., 2010). This algorithm corrects for atmospheric effects and surface emissivity by applying a look-up table derived from global land surface emissivity data in the thermal infrared spectrum (Wan *et al*., 2002).

2.3. *Methodology*

This study employs a comprehensive approach to analyzing heatwave phenomena by integrating MODIS LST data with ground-based air temperature observations. As clear-sky conditions are a prerequisite for heatwave identification, particular attention was given to cloud cover in the analysis. A comparative assessment was conducted between MODIS daytime daily LST data and maximum air temperature measurements from 15 meteorological stations. In Fig. 2, several important aspects are illustrated: (a) a comparison is made between land surface temperature (LST) and air temperature, highlighting the variations and differences observed; (b) the relationship between LST and air temperature is analyzed through a linear regression model, demonstrating how predicted LST values correlate with actual air temperature readings; (c) data collected from 15 different ground-based monitoring stations is graphically represented, showing the recorded values of both LST and air temperature for a comprehensive analysis.

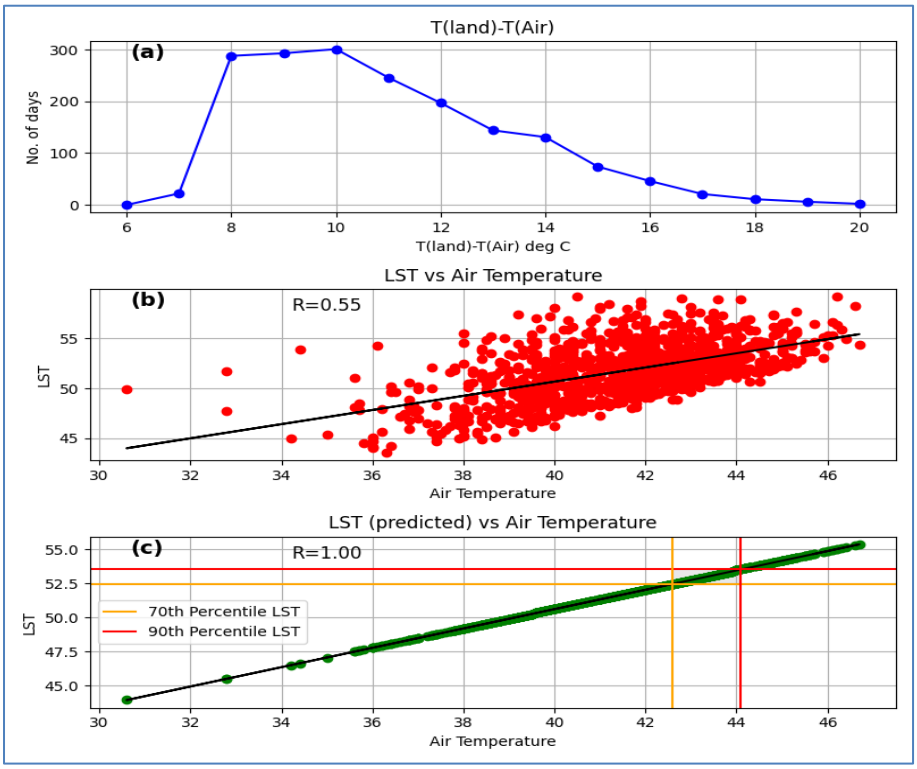

Figs. 2(a-c) (a) the difference between LST and air temperature is shown; (b) based on a linear regression model, the predicted LST values are correlated with the air temperature; (c) the LST and air temperature from 15 ground-based stations are plotted

To ensure methodological robustness, the study implemented the following three-step process:

Data Extraction: LST values were extracted from MODIS pixels corresponding to the geographical locations of the 15 meteorological stations.

Outlier Removal: Observations with discrepancies exceeding 7 °C between IMD air temperature data and MODIS-derived LST were excluded to retain only clear-sky observations. Additionally, air temperature readings above 40 °C were filtered to ensure the dataset captured relevant heatwave events.

Hybrid Algorithm: A novel approach was developed to combine MODIS LST data with air temperature observations for heatwave detection. This method involved calculating grid-based LST values to construct a spatial representation of heatwave dynamics across the study area.

The analysis was conducted using MODIS daytime LST data spanning from 2003 to 2020, focusing on the heatwave-prone months of March to June. The dataset was analysed on a high-resolution 2 km × 2 km grid, enabling an in-depth assessment of heatwave patterns.

Thresholds Based on Percentiles: To quantify heatwave intensity and frequency, the study established temperature thresholds based on daily LST percentiles ranging from the 50th to the 95th percentile. Additionally, the Excess Heat Factor Index was employed by overlaying maximum temperature contours obtained from MODIS data with IMD gridded air temperature data to enhance validation.

Relative Humidity and Synoptic Conditions: Further analysis incorporated the role of surface relative humidity and synoptic wind conditions at 850 hPa to assess their influence on heatwave exposure and thermal comfort levels. Given that the Terra satellite's overpass occurs near peak daily air temperature, the correlation between LST and air temperature readings was significantly enhanced. An examination of daily LST trends from March to June revealed distinct heatwave patterns, with notable spatial and temporal variations in intensity and prevalence. The analysis of relative humidity highlighted its substantial impact on thermal discomfort during heatwave events, particularly when coupled with prevailing wind conditions.

By integrating MODIS LST data with air temperature observations, this study provides

TABLE 1

The number of heat wave events over west Madhya Pradesh from 2009 to 2020

S No.	Year	Months	Duration
1	2009	May	17-19
2	2010	May	24
3	2011	May	23-29
4	2012	April	3-5, 8-11
		May	26-28
5	2013	May	18-26
6	2014	May	23, 29-30
		June	2, 4, 5, 6, 7-9, 11
7	2015	May	17-21, 23-24
8	2016	March	25-26
		May	13, 15-20
		June	07-09
9	2017	March	26-31
		April	3-4, 15-21
		May	13-14, 17
10	2018	May	19, 22-29, 31
11	2019	May	29-31
		June	03-12,
12	2020	May	22-25, 27

a comprehensive understanding of heatwave dynamics, particularly in regions with sparse meteorological coverage. The inclusion of relative humidity and synoptic wind patterns further refines the assessment of heatwave impacts on human thermal comfort and regional vulnerability, contributing to improved preparedness and mitigation strategies. The hybrid approach developed in this study has broad applications, including urban heat island research, climate adaptation planning, and early warning system development for extreme heat events. By leveraging satellite data and advanced algorithms, this methodology effectively bridges gaps in heatwave detection, offering valuable insights into their spatio-temporal variability and associated risks.

2.4. *Mechanism of heatwave*

For the formation and sustenance of heat waves, there are some favorable conditions such as:

(*i*) The region should have warm and dry air with an appropriate flow of hot air from the adjoining areas, (*ii*) Little or no moisture present in the upper air, (*iii*) Cloudless sky to allow maximum incoming solar radiation, (*iv*) Nearly dry adiabatic lapse rate, (*v*) There should be a well-defined ridge over the mid-troposphere region to allow air subsidence.

2.5. *Criteria for detection of heat wave in air temperature*

According to Indian Meteorological Department (IMD), heat wave is defined as, when maximum temperature (T*max*) of a station reaches ≥40 °C for plains and ≥30 °C for hilly regions. Also, there are three different categories based on which the following criteria

(*i*) Based on departure from normal, (a). Departure of T_{max} from normal is 4.5-6.4°C: heat wave, (b). Departure of T_{max} from normal is ≥6.5 °C: severe heat wave

(*ii*) Based on actual maximum temperature, (a). When actual T_{max} ≥45 °C: heat wave, (b). When actual T_{max} ≥ 47° C: severe heat wave

(*iii*) Criteria for heat wave for coastal stations (a). When the departure of actual T_{max} from normal is greater than 4.5 °C.

3. Results and discussion

3.1. *Heatwave detection criteria adopted using LST*

This study utilized MODIS Land Surface Temperature (LST) data as a proxy for heatwave detection, integrating it with ground-based ambient air temperature measurements. While air temperature data are traditionally employed to identify heatwaves, their relatively low spatial resolution limits their effectiveness for regional-scale analyses. In contrast, LST has been established as a reliable indicator for heatwave studies (Kawashima *et al*., 2000; Good *et al*., 2017; Bahi *et al*., 2016). To enhance detection accuracy, a hybrid algorithm combining LST and air temperature data was developed to establish heatwave detection thresholds.

A detailed analysis was conducted on 33 heatwave (HW) events, with a particular focus on western Madhya Pradesh, a region in central India known for frequent heatwave occurrences, especially during summer. The geographical location of this region-positioned between an arid zone to the west and a forested area to the east-makes it an optimal site for studying heatwave movement and propagation. This transitional zone provides a unique opportunity to trace the progression of heatwaves from source regions (arid zones) to sink regions (cooler, forested zones), thereby highlighting temperature gradients and movement dynamics. Understanding these patterns can aid meteorologists in predicting heatwave propagation and its associated impacts.

Table 1 summarises the 33 identified heatwave events between 1979 and 2020, providing details on their dates, years, and months of occurrence. This summary offers insights into the temporal distribution and evolution of heatwaves over the study period and serves as a foundation for the subsequent analyses presented in the results section.

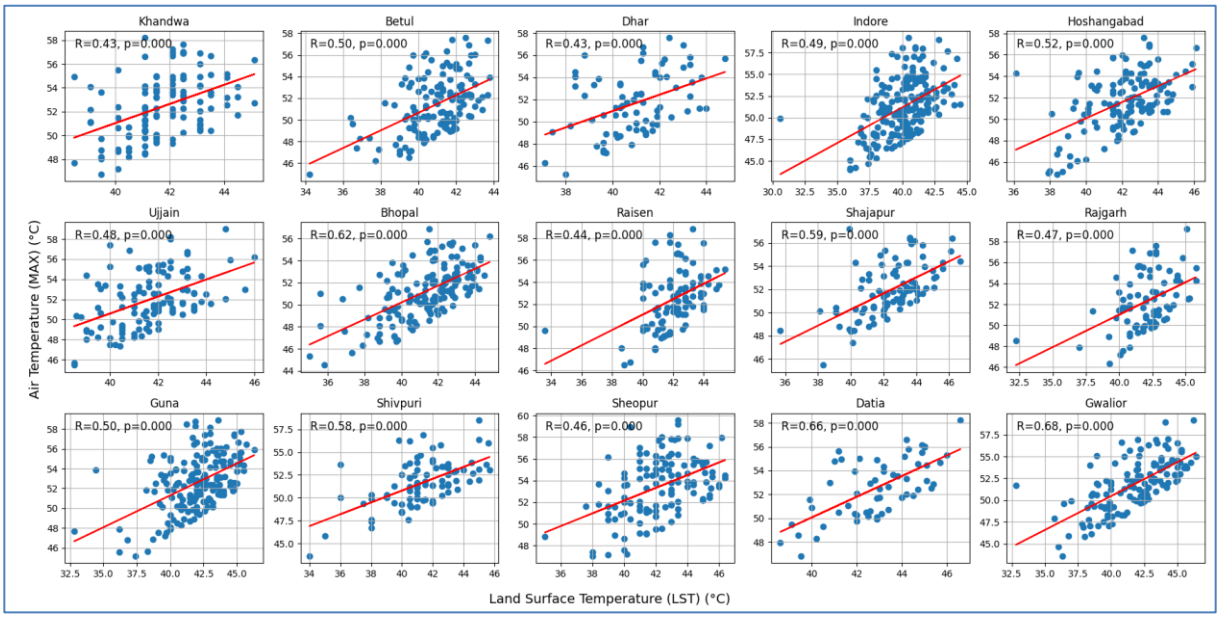

Fig. 3. The relationship of Air Temperature (Tair) from individual ground-based IMD stations located over western Madhya Pradesh with the LST from MODIS for May months over 2009-2020 with correlation coefficients and p-values denoted in each

To examine the spatial and temporal variability of heatwaves, freely available MODIS LST data were accessed via the Google Earth Engine (GEE) platform for western Madhya Pradesh. A gridded analysis was conducted at a spatial resolution of 2 km × 2 km, enabling the identification of heatwave duration, frequency, and intensity. This approach provides a comprehensive assessment of heatwave dynamics, contributing to a more refined understanding of their impacts in the region.

3.2. *Comparison of heat wave events from LST and air temperature*

The relationship between Land Surface Temperature (LST) and ambient air temperature (T_air) was analysed across two agro-meteorological eco-regions in western Madhya Pradesh (WMP). Fig. 3 illustrates how environmental, topographic, and methodological factors influence this relationship. Pearson correlation coefficients (R) between LST and T_air were calculated using data from 15 ground-based meteorological stations operated by the India Meteorological Department (IMD), covering the period from May 2009 to 2020.

The analysis revealed that increased terrain roughness weakens the LST-T_air correlation. For instance, stations in the southern Deccan Plateau exhibited moderate correlations, with R values of 0.43 in Khandwa, Betul, and Dhar, likely due to of high solar insolation with mountainous terrain. Urban areas demonstrated notable effects on the LST-T_air relationship due to the Urban Heat Island (UHI) phenomenon. In major cities such as Indore (R = 0.49) and Ujjain (R = 0.48), the replacement of natural vegetation with impervious surfaces contributed to elevated surface temperatures. In contrast, regions with significant forest cover, such as Bhopal and Hoshangabad, exhibited reduced UHI effects, with correlation coefficients exceeding 0.5.

Northern parts of the state, including Gwalior (R = 0.68) and Datia (R = 0.66), demonstrated the strongest correlations between LST and T_air. These areas are characterised by relatively flat terrain, which likely enhances consistency between surface and air temperature measurements. Statistical significance was tested for all correlations, with p-values provided alongside the correlation coefficients in Fig. 2. A significant p-value greater than 99.xxxx percent confidence level was found in all cases, allowing for the rejection of the null hypothesis (H_0) and confirming a statistically significant relationship between maximum air temperature and land surface temperature (LST).

The UHI effect, particularly pronounced in densely populated urban areas, results from the replacement of natural vegetation with impervious surfaces such as buildings and roads, leading to local microclimate alterations. The combined impact of UHI and heatwaves in urban regions exacerbates thermal discomfort and stress among residents (Lee *et al*., 2017; Steeneveld *et al*., 2011), increasing their vulnerability to heat-related risks.

A widely used approach for detecting seasonal heatwave trends involves percentile-based threshold

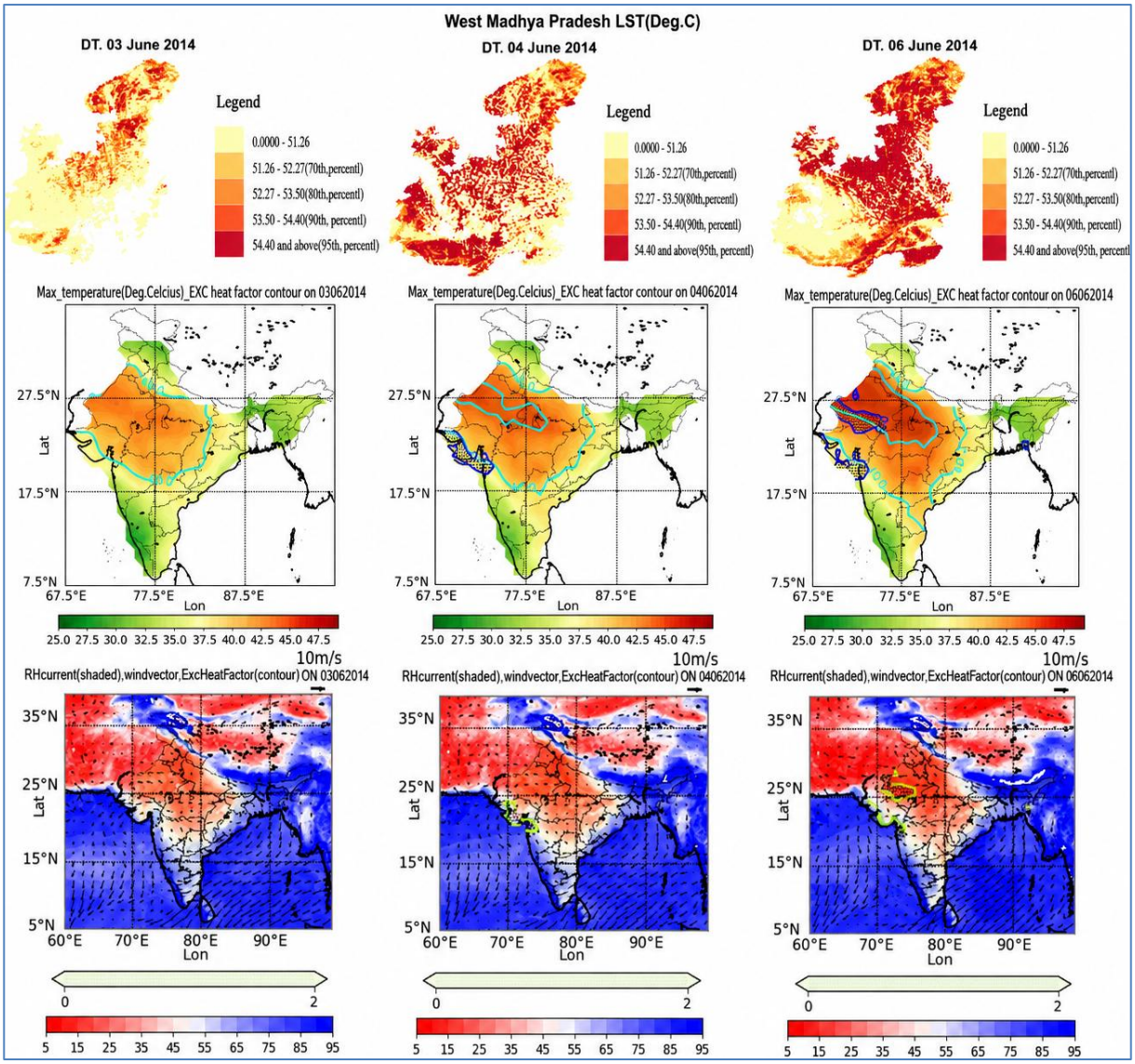

Fig. 4. Distribution of LST (MODIS) and Air Temperature (IMD gridded dataset) for the heat wave event of 04 June 2014

temperatures. This method entails calculating the 70th and 90th percentiles of LST values over a specific period (*e.g.*, a month) and using these thresholds to identify heatwave conditions. For instance, defining a heatwave as a period when at least 50% of the area exhibits LST values above the 70th percentile enables the analysis of seasonal heatwave trends across western Madhya Pradesh. This approach facilitates a more comprehensive understanding of heatwave patterns, contributing to improved climate adaptation strategies and risk mitigation efforts.

3.3. *Heat wave patterns observed from LST and air temperature in 2014*

Fig. 4 illustrates the Land Surface Temperature (LST) variation over the study region on June 3, 4, and 6, 2014, highlighting dynamic patterns influenced by environmental and meteorological factors. On June 3, the LST exhibited distinct spatial heterogeneity. Urban areas showed significantly higher temperatures compared to cooler regions, such as vegetated landscapes and water bodies. This pattern is indicative of the Urban Heat Island (UHI) effect, wherein built-up areas retain more heat due to reduced vegetation and impervious surfaces (Mora *et al*., 2017; Dosio *et al*., 2018). By June 4, a notable increase in LST was observed across various land cover types. This rise was likely driven by solar radiation and changing atmospheric conditions, suggesting a transitional phase where the environment begins responding to evolving meteorological parameters. On June 6, the LST distribution showed a further increase, signifying intensified terrestrial radiation combined with prolonged

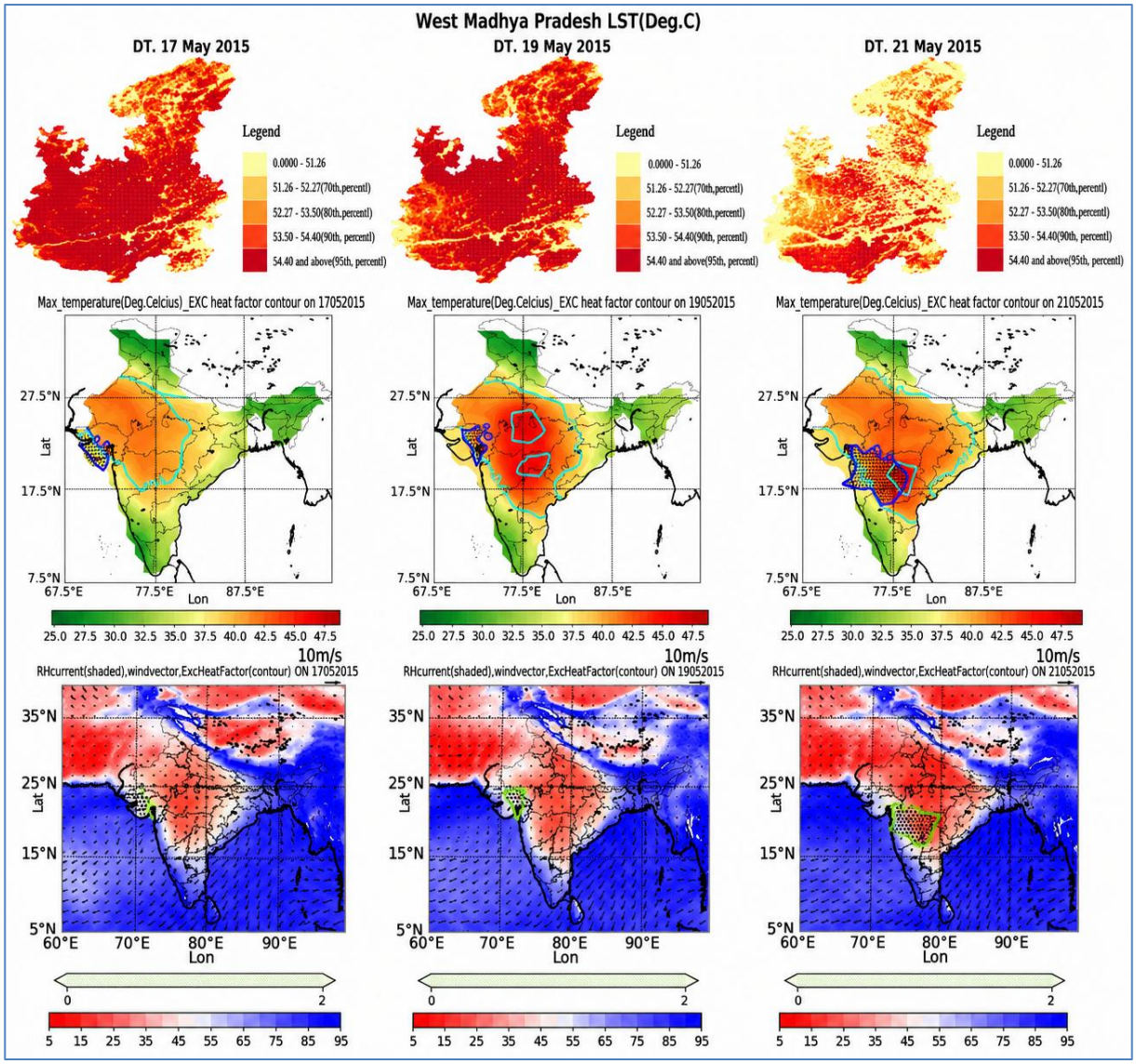

Fig. 5. LST (Land Surface Temperature) distribution and Air Temperature over Madhya Pradesh for 19 May 2015

solar insolation. These temporal and spatial variations in LST highlight the importance of monitoring surface temperature to understand local climate dynamics and identify potential heatwave hotspots.

The middle row of Fig. 4 represents maximum temperature variations across the region. Notably, the latitude range between 17.5° N and 27.5° N was marked by heightened temperature conditions. However, while the LST patterns were well-defined, corresponding air temperature variations remained less pronounced until June 6, when a clearer correlation emerged. The third row depicts airflow patterns, which revealed a significant influx of hot winds from the northwest. This airflow pattern was a major driver of the heatwave events observed on June 4 and 6, contributing to the thermal stress experienced in the region. This analysis underscores the value of LST in capturing the spatial and temporal dynamics of heatwaves and their interactions with atmospheric conditions, providing crucial insights for identifying and managing heatwave hotspots effectively.

3.4. *Heatwave patterns observed from LST and air temperature in 2015*

Fig. 5 illustrates the progression of heatwave conditions on May 17, 19, and 21, 2015, based on Land Surface Temperature (LST) data from MODIS. The analysis reveals a clear intensification of thermal stress across the study region during this period. On May 17, an initial surge in LST was observed, particularly in urban and densely built-up areas, marking the early onset of

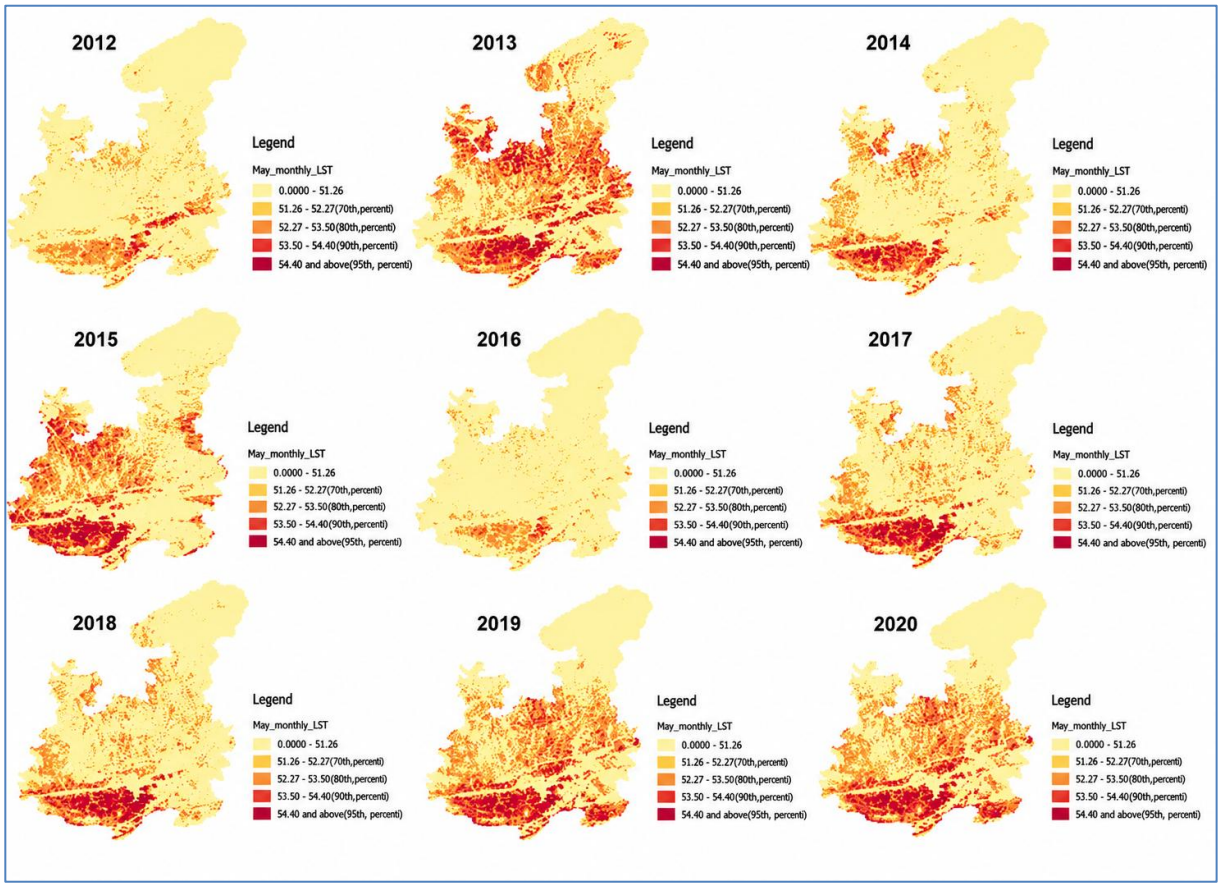

Fig. 6. Physiographical distribution of Heatwave areas as reflected from LST in May from the period 2012 to 2020

elevated temperatures. By May 19, LST values had risen significantly, covering a broader geographical area. The persistence of heightened temperatures indicated the intensification of the heatwave, likely influenced by atmospheric conditions, prolonged solar exposure, and anthropogenic factors (Chaturvedi *et al*., 2012; Narkhede *et al*., 2022). By May 21, although LST values began to normalise, the widespread effects of the heatwave remained evident, highlighting the sustained nature of thermal stress.

The middle row of Fig. 5 presents the distribution of maximum temperatures. On May 17, peak temperatures reached approximately 42.5 °C in northern India. By May 19, temperatures in western Madhya Pradesh had risen to around 45 °C, marked by a heat stress contour (indicated in green). By May 21, the heatwave appeared to migrate southward, in alignment with changes in LST values depicted in the first row. The bottom row provides additional atmospheric context, displaying wind vectors and shaded relative humidity (RH). The prevailing northwesterly wind flow facilitated the advection of hot, dry air masses into the region, exacerbating heat conditions. Relative humidity remained low-a typical characteristic of heatwaves-further intensifying thermal stress. Additionally, the bottom row highlights Excess Heat Factor (EHF) values, which increased notably between May 17 and 19, particularly in western Madhya Pradesh. The alignment of these EHF values with LST and maximum temperature data underscores regions experiencing extreme heat, emphasising the severity of the heatwave during this period.

This comprehensive analysis highlights the interplay between atmospheric dynamics, land surface characteristics, and anthropogenic influences in shaping heatwave conditions and their intensification across the study region. Understanding these interactions is essential for improving heatwave prediction and mitigation strategies.

3.5. *Inter-annual characterization of heat waves hot spots in LST*

The analysis of Land Surface Temperature (LST) data for the study region from May 2012 to May 2020 reveals significant temporal variations, as illustrated in Fig. 6. Each sub-figure represents the monthly mean LST

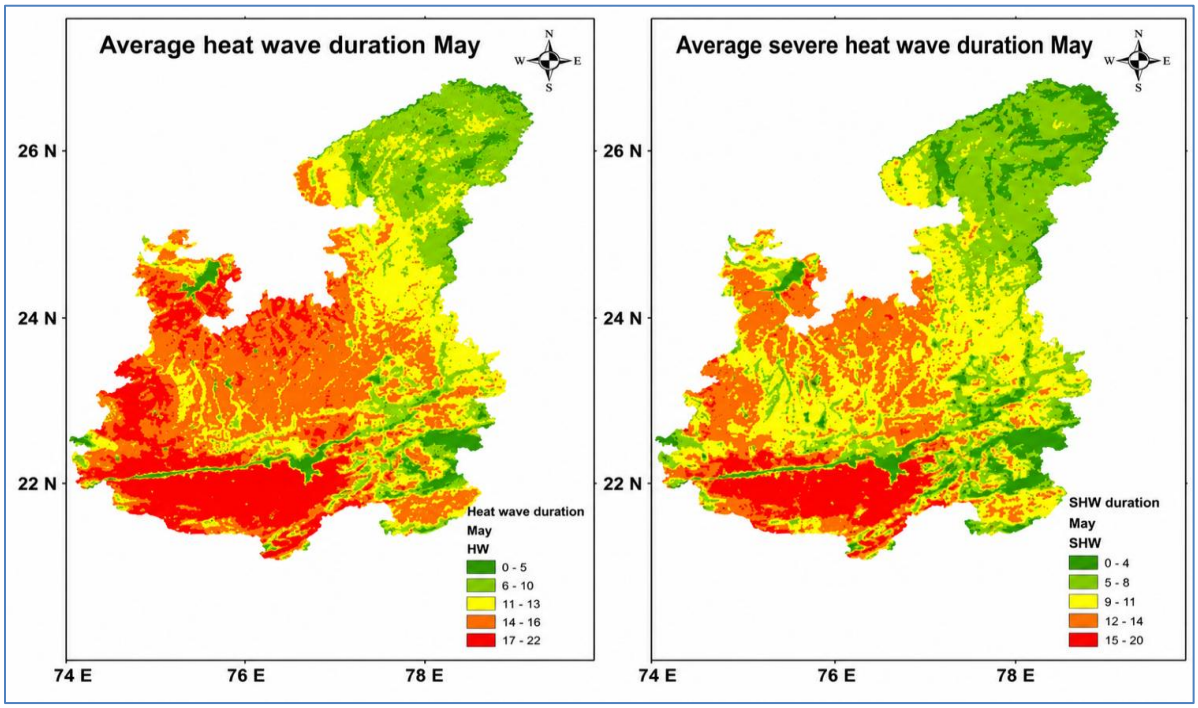

Fig. 7. Average duration of heat waves (HW) (70th percentile LST) and severe heat waves (SHW) (90th percentile LST) from 2012 to 2020 for May over Western Madhya Pradesh, India

for May of a specific year, providing valuable insights into the region's thermal dynamics and susceptibility to climatic shifts. In 2012, LST exhibited a relatively stable pattern, with only minor fluctuations observed along riverbed areas. However, by 2013, a subtle increase in LST was evident, suggesting an emerging shift in climatic conditions. This trend intensified notably in 2015, when a pronounced spike in LST was observed, coinciding with a significant heatwave that impacted the plateau region of the state. The year 2016 marked a return to relatively normal conditions, with LST values stabilising. However, in 2017 and 2018, elevated LST levels were recorded, particularly over the southwestern plateau region, indicating a sustained warming trend. Patterns for 2018 and 2019 continued to show heightened LST values with intermittent deviations, suggesting ongoing climatic fluctuations. By 2020, the data indicate a potential adaptation of the region to varying environmental influences, with LST trends reflecting broader climatic patterns.

This temporal analysis underscores the utility of LST in monitoring the thermal dynamics of the area and highlights its role as a complementary tool to air temperature data for heatwave detection. These findings align with previous studies (Zhang *et al*., 2016; Mora *et al*., 2017), offering a comprehensive perspective on the region's vulnerability to climate fluctuations. The ability to detect year-on-year variations in LST enhances its application as a key tool for assessing heatwave patterns and informing climate adaptation strategies.

3.6. *Decadal distribution of heat wave and severe heat wave days over the study region in may*

Fig. 7 illustrates the variation in heat wave (HW) and severe heat wave (SHW) durations during May, averaged from 2012 to 2020, based on Land Surface Temperature (LST) data. The findings indicate that the study region experienced prolonged HW and SHW conditions, with varying durations. Notably, areas with higher urban development, particularly in the central region, exhibited more pronounced heat wave occurrences. In contrast, forested areas in the northeast displayed minimal heat wave activity, likely due to differences in radiation balance.

The analysis reveals that heat waves in May extended up to 22 days, suggesting a prolonged period of elevated temperatures that may impact local ecosystems, agriculture, and human health. Severe heat waves persisted for a maximum of 20 days, further intensifying thermal stress in the region. These prolonged episodes highlight an increasing frequency of extreme temperature events in May, potentially driven by broader climatic trends and anthropogenic influences. Continuous monitoring of LST in conjunction with air temperature data is essential for developing adaptive strategies to mitigate the adverse effects of extreme heat.

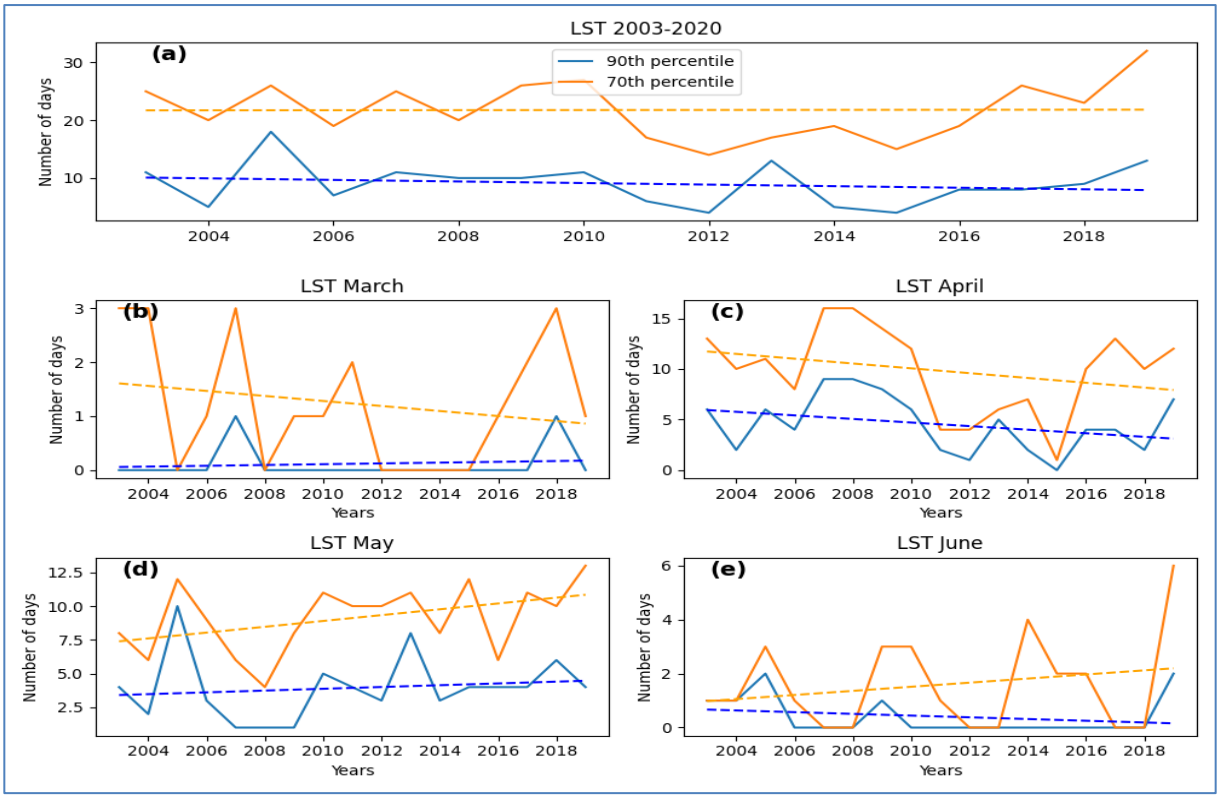

Figs 8(a-e). (a): Number of HW days from the 70th and 90th percentile LST over the study region for March, April, May, and June combined for 2003-2020; (b-e) represents the number of days from the 70th and 90th percentile LST in March, April, May, and June separately from 2003-2020

3.7. *Decadal distribution of heatwave and severe heatwave days*

Fig. 8 presents the seasonal trends of heat waves from March to June over the period 2003-2020, revealing distinct patterns in LST variations. Fig. 8(a) illustrates the mean LST changes over these months, highlighting seasonal transitions. In March, the onset of spring is marked by a gradual temperature rise. By April, heat wave occurrences become more frequent as temperatures continue to increase. In May, heat waves intensify, marking the transition into summer, with LST peaking during this month. June represents the peak of the spring-to-summer transition, characterised by the highest frequencies of heat waves and maximum LST values. This seasonal analysis provides insight into the evolution of temperature extremes from early spring to early summer over the study period.

Figs. 8(b-e) further analyse heat wave trends from 2003 to 2020, focusing on March, April, May, and June. The data highlight LST patterns at the 70th and 90th percentiles. The 70th percentile LST (52.5 °C) consistently indicates higher temperatures during heat wave events, suggesting extended HW durations. Conversely, the 90th percentile LST (53.5 °C) reflects a broader range of temperature variability, associated with shorter SHW durations (Rohini *et al.*, 2016; Oyler *et al.*, 2016). These findings indicate that while the region experiences SHW conditions, HWs tend to be longer in duration, with sustained heating at the 70th percentile threshold. The subplots offer valuable insights into the intensity and extent of extreme heat, as measured by LST, over the studied period.

3.8. *Discussions*

Ground-based observations of ambient temperature are the most commonly used data for studying heatwaves (Mishra *et al.*, 2017; Papanastasiou *et al.*, 2014). However, these measurements lack the spatial granularity required for disaster risk reduction, as they do not provide fine-scale (~2 km) spatial variability. An alternative dataset that addresses this limitation is the Moderate Resolution Imaging Spectroradiometer (MODIS) Land Surface Temperature (LST) dataset, which has provided continuous daily day- and night-pass data at a 1-km resolution since 2003 (Bahi *et al.*, 2016). Several studies have demonstrated a strong correlation between LST and ambient temperature (Good *et al.*, 2017; Kawashima *et al.*, 2000; Bahi *et al.*, 2016). In this study, a correlation coefficient exceeding 0.5 was obtained for most of the

stations analyzed (Fig. 3), suggesting that MODIS LST can serve as a reliable proxy for ambient air temperature in examining the spatio-temporal characteristics of heatwaves at a local scale.

Heatwave frequency in India has increased significantly, rising from 25 events in the period 1981-1990 to 67 in 2001-2010 (IMD, 2019; Rohini *et al*., 2016). This trend is exacerbated by rapid urbanization and changes in land use and land cover (LULC) (Rathee, 2014; Geetika, 2014). Figs. 4 and 5 indicate that land cover characteristics, particularly vegetation type, cropping patterns, and changes in built-up areas, play a critical role in the spatial distribution of heatwave hotspots. The study region is predominantly covered by dry deciduous forests, which remain leafless from April to June (Roy *et al*., 2012). Additionally, the widespread presence of rainfed cropland (Kharif) results in large areas of fallow land during the peak summer months (April–June). These conditions create a landscape with minimal green cover and reduced evapotranspiration, leading to high temperatures with limited moderation. This pattern is particularly pronounced in the southern and western parts of the study area (Fig. 6).

Urbanization has further intensified warming trends by reducing permeable surfaces, increasing albedo, and consequently elevating temperatures. Due to the limited coverage of ground-based temperature observations, MODIS LST data have been widely used as a substitute for ambient air temperature measurements. While LST does not always accurately reflect actual ambient temperatures-particularly in non-vegetated areas where it tends to be higher-it remains a valuable tool for analyzing spatial temperature variations. Previous studies have successfully applied LST in heatwave research for cities such as Bhopal, Hoshangabad, and Gwalior (Bahi *et al*., 2016; Good *et al*., 2017; Kawashima *et al*., 2000). Nonetheless, an expanded network of ground-based observations would improve modelling accuracy, enabling better projections and pattern identification.

Seasonal and monthly variations in LST, as illustrated in Figs. 8(a-e), are influenced by several meteorological factors, including wind speed, cloud cover, climatology, and atmospheric stability. Additionally, significant spatial differences in LST have been linked to the effects of El Niño and La Niña (Yan *et al*., 2020). The expansion of impervious surfaces in urban areas has also contributed to rising surface temperatures, altering surface radiation and moisture dynamics (Tian *et al*., 2021). The Urban Heat Island (UHI) effect, driven by dense high-rise buildings, heat-absorbing artificial materials, reduced vegetation cover, anthropogenic heat emissions, disrupted urban ventilation, and air pollution, further exacerbates urban temperature increases (Steeneveld *et al*., 2011; Mirzaei, 2015; Aleksandrowicz *et al*., 2017; Palme *et al*., 2017; He, 2019). Land cover composition is critical in determining UHI intensity, with the relationship between LST and the Normalised Difference Vegetation Index (NDVI) serving as a key indicator of land cover changes (Singh & Grover, 2015). LST, and atmospheric temperature remain among the most widely used indices for assessing UHI effects (Sheng *et al*., 2017; Eludoyin *et al*., 2019; Sun *et al*., 2020; Tian *et al*., 2021).

4. Conclusions

Analysis of LST in western Madhya Pradesh across daily (Figs. 4 and 5), monthly over a nine-year period (Fig. 6), and yearly (Figs .7 and 8) timescales confirms the efficacy of satellite-based LST in detecting regional heatwave patterns. A strong correlation (correlation coefficient, CC $\geq$ 0.5) was found between heatwaves identified through IMD air temperature anomalies and those estimated using LST anomalies. The study establishes optimal LST thresholds for heatwave detection: 52.5 °C (70^{th} percentile) for standard heatwaves and 53.5 °C (90^{th} percentile) for severe heatwaves. Additionally, an LST exceeding 47 °C, combined with a temperature anomaly of 4-5 °C, is proposed as an effective threshold for identifying heatwave conditions over inland stations.

The findings further underscore that summer warming trends in northern and central India have significantly increased the frequency, intensity, and duration of heatwaves over the past decade (Rao *et al*., 2021). Yearly heatwave patterns are well captured at a monthly scale in LST data, providing valuable insights into temporal and spatial variability. However, the study highlights the need to refine regional coefficients of LST anomalies to improve alignment with air temperature methodologies. This suggests that further research is required to enhance the integration of these complementary approaches.

In conclusion, satellite-derived LST data have proven to be a reliable and valuable resource for detecting and monitoring heatwaves, particularly in the context of rising temperatures and their growing environmental and human health impacts. The integration of LST data with traditional air temperature observations can strengthen early warning systems and contribute to more effective heatwave mitigation strategies.

Acknowledgment

The authors acknowledge Head, MTI, Pune, for his support. Authors acknowledge encouragement and

support by Head, CRS, Pune. The authors are thankful to the DGM, IMD for his encouragement and support. The authors are thankful to the NDC, IMD for providing gridded temperature data for the study region.

Authors' contributions

Gauravendra. P. Singh: Conception and design of the study and provision of data, revision of the manuscript.
Adarsh Dube: design of the study, writing first draft, data analysis, methodology (*email: adarsh.dube92@gmail.com*).
Neetin Narkhede: Data analysis: (*email:narkhedenm71@yahoo.co.in*).
G. K. Sawaisarje: revision, writing review and editing, supervision.(*email*: *gksawaisarje@gmail.com*)

Disclaimer: The contents and views expressed in this research article are the views of the authors and do not necessarily reflect the views of the organizations they belong to.

References

Albright, T. P., Pidgeon, A. M., Rittenhouse, C. D., Clayton, M. K., Flather, C. H., Culbert, P. D. and Radeloff, V. C., 2011, "Heat waves measured with MODIS land surface temperature data predict changes in avian community structure", *Remote Sensing of Environment*, **115**, 1, 245-254. https://doi.org/10.1016/j.rse.2010.08.024.

Aleksandrowicz, O., Vuckovic, M., Kiesel, K., Mahdavi, A., 2017, "Current trends in urban heat island mitigation research: Observations based on a comprehensive research repository", *Urban Climate*, **21**, 1-26. https://doi.org/10.1016/j.uclim.2017.04.002.

Bahi, H., Rhinane, H., Bensalmia, A., 2016, "Contribution of MODIS satellite image to estimate the daily air temperature in the Casablanca City, Morocco", *Int Arch Photogramm Remote Sens Spat Inf Sci - ISPRS Arch*, **42**, 2W1, 3-11. https://doi.org/10.5194/isprs-archives-XLII-2-W1-3-2016.

Barriopedro, D., Fischer, E. M., Luterbacher, J., Trigo, R. M., García-Herrera, R., 2011. The hot summer of 2010: redrawing the temperature record map of Europe. *Science*, 332(6026), 220-224, https://doi.org/10.1126/science.1201224.

Chaturvedi, R., Joshi, J., Jayaraman, M., Bala, G., Ravindranath, N., 2012. Multi-model climate change projections for India under representative concentration pathways. *Current Science*, 103(7), 791–802,

Dosio, A., Mentaschi, L., Fischer, E.M., Wyser, K., 2018. Extreme heat waves under 1.5 C and 2 C global warming. *Environmental research letters*, 13(5), 054006, https://doi.org/10.1088/1748-9326/aab827

Eludoyin, Adebayo & Omotoso, Iyanuoluwa & Eludoyin, Oyenike & Popoola, Kehinde. (2019). Remote Sensing Technology for Evaluation of Variations in Land Surface Temperature, and Case Study Analysis from Southwest Nigeria: Volume Eight. https://doi.org/10.1007/978-3-030-04750-4_8.

Findell, K.L., Berg, A., Gentine, P., Krasting, J.P., Lintner, B.R., Malyshev, S., Shevliakova, E., 2017. The impact of anthropogenic land use and land cover change on regional climate extremes. *Nature communications*, 8(1), 989. https://doi.org/10.1038/s41467-017-01038-w.

Good, E.J., Ghent, D. J., Bulgin, C. E., Remedios, J. J., 2017. A spatiotemporal analysis of the relationship between near-surface air temperature and satellite land surface temperatures using 17 years of data from the ATSR series. *Journal of Geophysical Research: Atmospheres*, 122(17), 9185-9210. https://doi.org/10.1002/2017JD026880.

He, B.J., Zhu, J., Zhao, D.X., Gou, Z.H., Qi, J.D., Wang, J. 2019. Co-benefits approach: Opportunities for implementing sponge city and urban heat island mitigation. *Land use policy*, 86, 147-157, https://doi.org/10.1016/j.landusepol.2019.05.003.

Jin, M., 2004, Analysis of land skin temperature using AVHRR observations. *Bull. Am. Meteorol. Soc*. 85, 587. https://doi.org/10.1175/BAMS-85-4-587.

Kawashima, S., Ishida, T., Minomura, M., Miwa, T., 2000. Relations between surface temperature and air temperature on a local scale during winter nights. *J Appl Meteorol* 39(9), 1570–1579, https://doi.org/10.1175/1520-0450(2000)039<1570:RBSTAA>2.0.CO;2 .

Knowlton K. et al., 2014. Ahmedabad Heat and Climate Study Group, Development and implementation of South Asia's first heat-health action plan in Ahmedabad (Gujarat, India). *Int. J. Environ. Res. Public Health*, 11, 3473–3492, https://doi.org/10.3390/ijerph110403473.

Lee, Y.Y., Din, M.F.M., Ponraj, M., Noor, Z.Z., Iwao, K., Chelliapan, S., 2017. Overview of urban heat island (UHI) phenomenon towards human thermal comfort. *Environmental Engineering & Management Journal (EEMJ)*, 16(9), https://doi.org/10.30638/eemj.2017.217.

Li Zhong Qiang, L.Z., He Liang, H.L., Zhang Huan, Z.H., Urrutia-Cordero, P., Ekvall, M.K., Hollander, J., Hansson, L.A., 2017. Climate warming and heat waves affect reproductive strategies and interactions between submerged macrophytes. *Glob. Change Biol*. 23, 108–116. https://doi.org/10.1111/gcb.13405.

Mildrexler, D.J., Zhao, M., Running, S.W. 2011. A global comparison between station air temperatures and MODIS land surface temperatures reveals the cooling role of forests. *J. Geophys. Res.-Biogeosci*. 116. https://doi.org/10.1029/2010JG001486.

Mildrexler, D.J., Zhao, M., Cohen, W.B., Running, S.W., Song, X.P., Jones, M.O., 2018. Thermal Anomalies Detect Critical Global Land Surface Changes. *J. Appl. Meteorol. Climatol*. 57, 391–411, https://doi.org/10.1175/JAMC-D-17-0093.1.

Mirzaei, P.A., 2015. Recent challenges in modeling of urban heat island. *Sustainable cities and society*, 19, 200-206, https://doi.org/10.1016/j.scs.2015.04.001.

Mishra, V., Mukherjee, S., Kumar, R., Stone, D.A., 2017. Heatwave exposure in India in current, 1.5 °c, and 2.0 °c worlds. *Environ Res Lett.*, 12(12). https://doi.org/10.1088/1748-9326/aa9388.

Mora, C., Dousset, B., Caldwell, I. R., Powell, F. E., Geronimo, R. C., Bielecki, C. R., Trauernicht, C., 2017. Global risk of deadly heat. *Nature climate change*, 7(7), 501-506. https://doi.org/10.1038/nclimate3322

Narkhede, N., Chattopadhyay, R., Lekshmi, S., Guhathakurta, P., Kumar, N., Mohapatra, M., 2022. An empirical model-based framework for operational monitoring and prediction of heatwaves based on temperature data. *Modeling Earth Systems and Environment*, 8(4), 5665-5682, https://doi.org/10.1007/s40808-022-01450-2.

Oyler, J. W., Dobrowski, S. Z., Holden, Z. A., Running, S. W., 2016. Remotely sensed land skin temperature as a spatial predictor of air temperature across the conterminous United States. *Journal*

of Applied Meteorology and Climatology, 55(7), 1441-1457, https://doi.org/10.1175/JAMC-D-15-0276.1

Pai, D. S., Smithaanil, N and Ramanathan, A. N., 2013. Long term climatology and trends of heat waves over India during the recent 50 years (1961–2010). *Mausam*, 64, 585–604, https://doi.org/10.54302/mausam.v64i4.742

Pal, Jeremy S., Elfatih A. B., 2016. Future temperature in southwest Asia projected to exceed a threshold for human adaptability. *Nature Climate Change*, 6.2, 197-200, http://dx.doi.org/10.1038/nclimate2833.

Palme, M., Inostroza, L., Villacreses, G., Lobato, A., Carrasco, C., 2017. Urban weather data and building models for the inclusion of the urban heat island effect in building performance simulation. *Data in brief*, 14, 671-675, https://doi.org/10.1016/j.dib.2017.08.035.

Papanastasiou D.K., Melas D, Kambezidis H.D., 2014. Heat waves characteristics and their relation to air quality in Athens. *Glob. Nest J* 16(5):919–928. https://doi.org/10.30955/gnj.001530.

Parmar, P.N., Pandya, M.R., Dave, J.A., Varchand, H.K., Trivedi, H.J., 2022. Heat Wave Study using Satellite LST and Air Temperature Data over Gujarat Region. In 2022 URSI Regional Conference on Radio Science (USRI-RCRS) (pp. 1-4). *IEEE*, https://doi.org/10.23919/URSI-RCRS56822.2022.10118491.

Perkins, S.E., 2015. A review on the scientific understanding of heat waves-Their measurement, driving mechanisms, and changes at the global scale. *Atmos. Res*. 164–165, 242–267. https://doi.org/10.1016/j.atmosres.2015.05.014.

R. Geetika, "Trends of Land-Use Change in India in Urbanization in Asia: Governance, Infrastructure and the Environment", *Springer* India, New Delhi, pp. 215—238, 2014, https://doi.org/10.1007/978-81-322-1638-4_13.

Rao, P., Gupta, K., Roy, A., Balan, R., 2021. Spatio-temporal analysis of land surface temperature for identification of heat wave risk and vulnerability hotspots in Indo-Gangetic Plains of India. *Theoretical and Applied Climatology*, 146(1-2), 567-582, https://doi.org/10.1007/s00704-021-03756-0

Rathee G., 2014. Trends of land-use change in India. In Urbanization in Asia: Governance, Infrastructure and The Environment (pp. 215–238). https://doi.org/10.1007/978-81-322-1638-4_13

Ribeiro, A. F., Russo, A., Gouveia, C. M., Pires, C. A., 2020. Drought-related hot summers: A joint probability analysis in the Iberian Peninsula. *Weather and Climate Extremes*, 30, 100279, https://doi.org/10.1016/j.wace.2020.100279

Robine, J.M., Cheung, S.L.K., Le Roy, S., Van Oyen, H., Griffiths, C., Michel, J.P., Herrmann, F.R., 2008. Death toll exceeded 70,000 in Europe during the summer of 2003. *Comptes Rendus. Biologies*, 331(2), 171-178, https://doi.org/10.1016/j.crvi.2007.12.001

Rohini, P., Rajeevan, M., Srivastava, A. K., 2016. On the variability and increasing trends of heat waves over India *Sci. Report*. 6 26153, https://doi.org/10.1038/srep26153

Roy S, Byrne J, Pickering C., 2012. A systematic quantitative review of urban tree benefits, costs, and assessment methods across cities in different climatic zones. *Urban Green* 11(4):351–363. https://doi.org/10.1016/j.ufug.2012.06.006

Russo, A., Gouveia, C.M., Dutra, E., Soares, P.M.M., Trigo, R.M., 2019. The synergy between drought and extremely hot summers in the Mediterranean. *Environmental Research Letters*, 14(1), 014011, https://doi.org/10.1088/1748-9326/aaf09e

Sheng, L., Tang, X., You, H., Gu, Q., Hu, H., 2017. Comparison of the urban heat island intensity quantified by using air temperature and Landsat land surface temperature in Hangzhou, China. *Ecological Indicators*, 72, 738-746, https://doi.org/10.1016/j.ecolind.2016.09.009.

Sjoukje. Y. Philip, Kew, S. F., van Oldenborgh, G. J., Anslow, F. S., Seneviratne, S. I., Vautard, R., Coumou, D., Ebi, K. L., Arrighi, J., Singh, R., van Aalst, M., Pereira Marghidan, C., Wehner, M., Yang, W., Li, S., Schumacher, D. L., Hauser, M., Bonnet, R., Luu, L. N., Lehner, F., Gillett, N., Tradowsky, J. S., Vecchi, G. A., Rodell, C., Stull, R. B., Howard, R., and Otto, F. E. L.: Rapid attribution analysis of the extraordinary heat wave on the Pacific coast of the US and Canada in June 2021, *Earth Syst. Dynam.*, 13, 1689–1713, https://doi.org/10.5194/esd-13-1689-2022

Singh, R. B., Grover, A., 2015. Spatial correlations of changing land use, surface temperature (UHI) and NDVI in Delhi using Landsat satellite images. *Urban development challenges, risks and resilience in Asian mega cities*, 83-97, https://doi.org/10.1007/978-4-431-55043-3_5

Snyder, W.C., Wan, Z., Zhang, Y., Feng, Y.Z., 1998. Classification-based emissivity for land surface temperature measurement from space. *International Journal of Remote Sensing*, 19(14), 2753-2774, https://doi.org/10.1080/014311698214497

Steeneveld, G.J., Koopmans, S., Heusinkveld, B.G., Van Hove, L.W.A., Holtslag, A.A.M., 2011. Quantifying urban heat island effects and human comfort for cities of variable size and urban morphology in the Netherlands. *Journal of Geophysical Research: Atmospheres*, 116(D20), https://doi.org/10.1029/2011JD015988.

Sun, Y., Wang, S., Wang, Y., 2020. Estimating local-scale urban heat island intensity using nighttime light satellite imageries. *Sustainable Cities and Society*, 57, 102125, https://doi.org/10.1016/j.scs.2020.102125

Tian, P., Li, J., Cao, L., Pu, R., Wang, Z., Zhang, H., Gong, H., 2021. Assessing spatiotemporal characteristics of urban heat islands from the perspective of an urban expansion and green infrastructure. *Sustainable Cities and Society*, 74, 103208, https://doi.org/10.1016/j.ecolind.2023.110057

Trenberth, Kevin E., John T. Fasullo., 2012. Climate extremes and climate change: The Russian heat wave and other climate extremes of 2010. *Journal of Geophysical Research: Atmospheres* 117.D17. https://doi.org/10.1029/2012JD018020

Vancutsem, C., Ceccato, P., Dinku, T., Connor, S.J., 2010. Evaluation of MODIS land surface temperature data to estimate air temperature in different ecosystems over Africa. *Remote Sensing of Environment*, 114(2), pp.449-465, https://doi.org/10.1016/j.rse.2009.10.002

Wan, Z., Zhang, Y., Zhang, Q., Li, Z.L., 2002. Validation of the land-surface temperature products retrieved from Terra Moderate Resolution Imaging Spectroradiometer data. *Remote sensing of Environment*, 83(1-2), 163-180, https://doi.org/10.1016/S0034-4257(02)00093-7

Yan, Y., Mao, K., Shi, J., Piao, S., Shen, X., Dozier, J., Bao, Q., 2020. Driving forces of land surface temperature anomalous changes in North America in 2002–2018. *Sci. Rep.*, 10, 6931. https://doi.org/10.1038/s41598-020-63701-5

Zhang, Y., Xiao, X., Zhou, S., Ciais, P., McCarthy, H., Luo, Y., 2016. Canopy and physiological controls of GPP during drought and heat wave. *Geophysical Research Letters*, 43(7), 3325-3333. https://doi.org/10.1002/2016GL068501

.